

# The Characteristic Time Scale of Cultural Evolution

Tobias Wand<sup>1,2\*</sup>

Daniel= Hoyer<sup>3,4</sup>

<sup>1</sup>Westfälische Wilhelms-Universität Münster, Insitut für Theoretische Physik

<sup>2</sup>Center for Nonlinear Science, Münster

<sup>3</sup> George Brown College, Toronto

<sup>4</sup> Evolution Institute, San Antonio

\* Corresponding Author: [t\\_wand01@uni-muenster.de](mailto:t_wand01@uni-muenster.de)

December 2022, Revised April 2023

## Abstract

Numerous researchers from various disciplines have explored commonalities and divergences in the evolution of complex social formations. Here, we explore whether there is a 'characteristic' time-course for the evolution of social complexity in a handful of different geographic areas. Time series data from the *Seshat: Global History Databank* is shifted so that the overlapping time series can be fitted to a single logistic regression model for all 18 geographic areas under consideration. To analyse the endogenous growth of social complexity, each time series is restricted to a central time interval without discontinuous polity changes. The resulting regression shows convincing out-of-sample predictions and its period of rapidly growing social complexity can be identified via bootstrapping as a time interval of roughly 800 years.

**Keywords:** Cliodynamics, Cultural Evolution, Time Scale

## 1 Introduction

### 1.1 Motivation to Find Characteristic Time Scales

Numerous researchers from various disciplines have explored commonalities and divergences in the evolution of complex social formations [1, 2, 3, 4, 5, 6, 7]. The recent emergence of Cliodynamics as a discipline has started the analysis of the dynamics of human societies and states with data-driven scrutiny and modelling approaches from natural sciences [8, 9]. Previous work established that a common set of factors associated with complex social formations typically moved in tandem across a wide variety of regions and time-periods; factors such as social scale, the use of informational media, administrative hierarchies, monetary instruments,

and others [6]. These were interpreted as comprising the primary dimension of what could be called 'social complexity' across cultures, though other dimensions can be adduced as well [3].

Various studies have already discussed or tried to identify the causal drivers of cultural evolution and evaluated the evidence for different theories of *why* cultures become more complex [7, 10, 11, 12, 13]. Beyond the *causal* similarities behind cultural evolution across cultures, researchers have also found evidence for *temporal* similarities and seemingly parallel time scales in the dynamics of various social structures. For example, models for societal collapse have been derived from demographic and fiscal data that show characteristic oscillation periods of few centuries and a fine structure with a faster periodicity of approximately two human generations [4]. Other theories suggest that cultural evolution leads to the emergence of similar political institutions and schools of thought at roughly identical time intervals across different geographic regions [14, 15, 16]. Another recent study has evaluated the connection between the first emergence of complex societies in different world regions and the age of widespread reliance on agriculture in those areas [17], supporting the theory that agriculture is a necessary condition for the evolution of complex societies. While the time lag between the primary reliance on agriculture and the emergence of states was found to decrease over time, an average time lag of roughly 3,400 years for pristine states suggested the existence of a characteristic time scale, though this was not the explicit focus of that study. Similarly, the study on causal drivers in [7] also found that the time since the adoption of agriculture had a statistically significant effect as a linear predictor variable (called 'AgriLag') for sociopolitical complexity, providing additional evidence for temporal regularities in the growth of complexity across different cultures and civilisations. Finally, using the same data as our article (cf. section 1.2), it was possible to identify periods of cultural macroevolution with either slow or rapid change in social complexity [5].

Nevertheless, as yet there is no consensus on whether there is a 'typical' time scale for sociopolitical development cross-culturally, let alone what that time-course might be. Such characteristic time scales of dynamic systems are, however, well documented in different areas of the natural sciences such as physics and chemistry [18, 19]. Differentiating between fast and slow time scales in a dynamical system can lead to useful insights [20]. In particular, Haken's theory of the 'enslaving principle' [21], according to which the dynamics of fast-relaxing modes are dominated (enslaved) by the behaviour of slowly relaxing modes in a dynamical system, pioneered the research on how dynamics on different time scales influence each other in the same observed system. The existence of temporal regularities among societal dynamics would suggest that cultural evolution not only occurs in similar developmental stages across geographic regions and time periods, but also in similar time intervals. This would add an important dimension to our understanding of *how* complex social formations evolve, and raise a number of critical questions about what drives these cross-cultural patterns.

Here, we adapt some of the methods employed in the natural sciences in an attempt to identify characteristic time scales in the evolution of complex societies. We utilise data collected by the *Seshat: Global History Databank* [22, 23, 24], a large repository of information collected about the dynamics of social complexity across world regions from the Neolithic to the early modern period [25]. We find that, despite significant differences in the timing and intensity of major increases in social complexity reached by polities across the Seshat sample, there is a typical, quantitatively identifiable time course recognisable in the data. This result is robust to a variety of checks and covers polities from all major world regions and across thousands of years of history. Our findings offer a novel contribution to the study of cultural evolution, indicating the existence of a general, cross-cultural pattern in both the scale as well as the pace of social complexity development.

## 1.2 Seshat Databank

The *Seshat: Global History Databank* includes systematically coded information on over 35 geographic areas and over 200 variables across up to 10,000 years in time steps of 100 years [22]. Note that this article analyses a previous data release with 30 Natural Geographic Areas (NGAs) spread across the globe to reduce possible geographic biases ([25]; see also publicly available data at <http://www.seshatdatabank.info/databrowser/>). During the time interval captured by the Seshat databank, these NGAs are occupied by 414 different identifiable polities, defined as an "independent political unit". This sample is constructed by identifying all known polities that occupied part or all of each NGA over time (see [22, 23, 24] for details). The recorded variables are aggregated to nine complexity characteristics (CCs) and a principal component analysis shows that 77% of the variation in the data can be explained by the first principal component SPC1, which has almost equal contributions from all nine CCs [6]. In the case of missing data or expert disagreement in [6], multiple imputation [26] was used to create several data sets with the differently imputed values which were aggregated into the principle component analysis. The NGAs in the Seshat data cover a wide geographical range and different levels of social complexity, though it is important to note that the Seshat sample is focused largely on relatively complex, sedentary societies (but not exclusively). Data on the CCs is sampled at century intervals, giving a time series of each polity's estimated social complexity measure throughout its duration.

Seshat data has allowed researchers to quantitatively test hypotheses on cultural evolution such as identifying drivers of social complexity and predictors of change in military technology, for example gauging the effect of moralising religions on cultural evolution or predicting historical grain yields [7, 27, 28, 29]. Further analysis of the Seshat data includes a discussion of ideas from biological evolutionary theory with respect to the *tempo* of cultural macroevolution,

defined as "rates of change, including their acceleration and deceleration", concluding that "cultural macroevolution is characterized by periods of apparent stasis interspersed by rapid change" [5]. These results strongly relate to the question of the present article, whether there is some generality in the time scale of cultural evolution in the Seshat data.

### 1.3 Data on Polity Boundaries and Duration

Each NGA's time series can contain data about very different polities that succeeded each other. Sometimes, a gradual and continuous change between the polities justifies treating predecessor and successor polities as closely related; for instance, in the Latium NGA (modern-day central Italy), Seshat records three separate polities for the Roman Republic, indicating the Early, Middle, and Late phases. These phases are culturally continuous, so here we record these as a single polity. In other cases, there may have been an invasion or mass migration as a clear break-point between the two polity's continuity; for instance, between the Ptolemaic Kingdom and Roman Principate polities in the Upper Egypt NGA. Data from [25] and other information recorded in the Seshat sample, notably information on the relationship between polities, is here used to establish a list of continuous polities. Specifically, we sub-sample polities that are coded as having 'continuity' in the variable *relationship to preceding (quasi)polity* (as opposed to codes of cultural assimilation, succession from another polity, large-scale population replacement, etc; see <https://seshatdatabank.info/methods/code-book/> for details).

### 1.4 Organisation of this Article

Section 2 explains how we transformed the time series data on each continuous polity in the Seshat sample to establish a common reference point to investigate the time course of changes in social complexity across NGAs. In short, we shift each NGA's time series with respect to a single anchor time such that the transformed time variable *RelTime* shows major overlap between the *RelTime*-vs-*SPC1*-curves of all NGAs. Exploratory data analysis for the whole dataset reveals that there is a logistic relationship between *RelTime* and the *SPC1* response variable. Motivated by these results, section 3 restricts each NGA's time series to its central part by using the knowledge about discontinuous polity changes as breakpoints. The goodness of fit is evaluated via an out-of-sample prediction and the characteristic time scale of the growth phase between the logistic function's plateaus is estimated via bootstrapping. Finally, the results of the analyses are summarised and discussed in section 4. The mathematical methods and technical details are discussed in the appendices A and B.

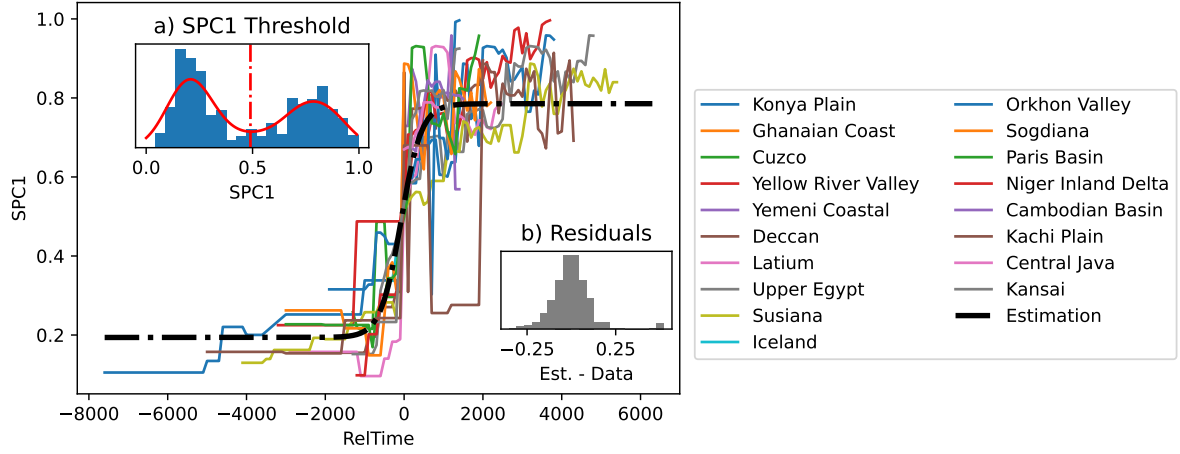


**Figure 1:** Main figure: Time series of RelTime vs. SPC1 for all 18 NGAs that cross  $SPC1_0$  and the logistic regression. Insets: a) distribution of SPC1 for all 30 NGAs, the associated KDE (red) and the threshold  $SPC1_0$  (vertical); b) residuals of the logistic regression.

## 2 Approach: Data Transformation and Exploratory Analyses

### 2.1 Anchor Time

Considering that most NGAs have an SPC1 time series that starts at a low value barely above 0 and ends at a high value close to 1, a logistic regression model seems like a reasonable suggestion for the data. Although all NGAs experience a growth in SPC1 over time, they start at very different calendar years. Therefore, it is necessary to shift the time series via an anchor time so that in the new "relative" time, the growth phase in each NGA's time series coincide. Then, one logistic regression can be used for all shifted time series (cf. A.1). Hence, each NGA  $i$  needs an anchor time  $T_a^{(i)}$  so that if all time series are shifted by  $-T_a^{(i)}$ , they roughly overlap. The anchor time can be chosen as the year during which the NGA  $i$ 's SPC1 value crosses a threshold value. It has already been shown that there is a clear threshold  $SPC1_0$  between high and low values of SPC1 in the data, which was used to define the *RelTime* variable in [28]. A similar methodology was also used in [30], but there, the authors used the emergence of a moralising religious belief as the "year zero" to shift each NGA's time series. Copying the procedure from [28] to get the *RelTime* variable,  $SPC1_0$  is chosen as the minimum between the two maxima in the kernel density estimation (KDE; explained in A.2) of the SPC1 values (figure 1, inset a). The anchor time  $T_a^{(i)}$  is then selected as the first recorded data point when the NGA  $i$  exceeds  $SPC1_0$ . An illustration of the anchor time shift is provided in the appendix B. Thus, the 12 NGAs that never exceed  $SPC1_0$  are discarded from this analysis. On the one hand, this is not too problematic because their limited growth in SPC1 means that they would have only contributed little information to the estimation of SPC1's characteristic growth time, but on the other hand, this discards all NGAs from the world regions North

America and Oceania-Australia in the Seshat sample, meaning that it might introduce a bias towards data from Afro-Eurasia. We discuss this and other possible limitations of the approach further in section 4.2 below.

## 2.2 Logistic Regression

The RelTime-vs-SPC1 data is fitted to a logistic regression curve (cf. A.1) via the optimisation algorithm *scipy.optimize.curve\_fit* from [31]. The shifted time series of the NGAs and the logistic fit are shown in the main part of figure 1. The quality of the regression curve is evaluated with the methods from A.3. With the exception of the outlier NGAs Kachi Plain and, to a lesser extent, the Yellow River Valley (we discuss these cases in section 3.2.1), all time series qualitatively agree with the regression curve. With few exceptions, the majority of the residuals shown in figure 1 (inset b) are distributed roughly symmetrically in a neighbourhood of zero. The distribution of the residuals and the rather low value of the root-mean-square-error  $RMSE \approx 0.11$  both indicate that the logistic regression is a suitable model for the shifted SPC1 data.

## 3 Results: Time Scales in the Evolution of Social Complexity

### 3.1 Fitting the Logistic Curve to Continuous Polities

There are two reasons why it makes sense to restrict the logistic regression only to a central part of each NGA’s time series, during which the polities in that NGA are not disrupted by external influence. First, the logistic regression starts at a plateau of low values of SPC1 close to 0 and ends at a plateau of high values close to 1. Therefore, even a bad interpolation for the central part can achieve a good  $RMSE$ , if the plateaus of the high and low tails are sufficiently accurate. However, this would not be a reliable estimation to make an inference on the growth phase in the centre of the curve. Second, if the NGA’s polity is e.g. annexed by another, more developed polity, then it inherits the invading polity’s high SPC1 value and may make a sudden jump in the SPC1 curve. However, the logistic regression here is intended to model endogenous growth like in [32] and not exogenous influences. Therefore, it makes sense to divide each NGA’s time series into intervals which are separated by sharp, discontinuous political changes within each NGA and to restrict the analysis of the NGA to its central interval, i.e. to the time series from the polities that cross the  $SPC1_0$  threshold.

To break the time series into intervals, data from [25] (supplemented with authors’ calculations [33]) is used to explain the relationships between the different polities that populate an individual NGA over the course of time. As a very broad distinction, the detailed information in this data is grouped into either continuous or discontinuous transitions (the latter includes every transition that is not categorised as continuous in the data). This process is illustrated with an example in the appendix B. Again, a logistic curve is fitted for each of the previous 18

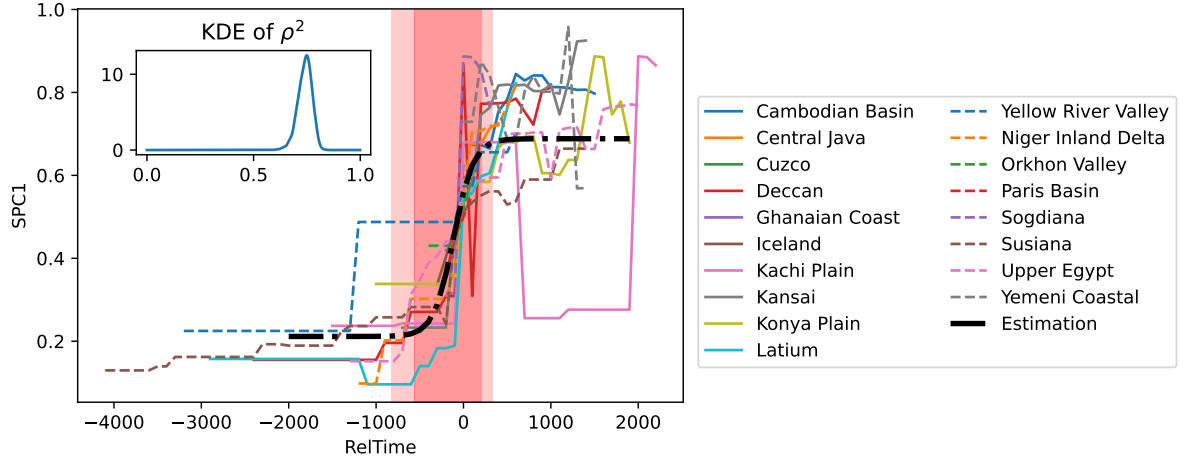


**Figure 2:** Main figure: Central part of the time series of RelTime vs. SPC1 for all 18 NGAs that cross  $SPC1_0$  and the logistic regression. The red area marks the period of growth of the logistic curve with light red being the respective uncertainty measures. Inset: KDE of the coefficient of prediction  $\rho^2$  for 1000 out-of-sample predictions with the logistic model.

Parameter	$a$	$b$	$c$	$d$
Estimation	0.48	0.21	44.0	-0.023
90% CIs	[0.39, 0.58]	[0.17, 0.25]	[18.8, 186.4]	[-0.034, -0.014]

**Table 1:** Parameters of the logistic regression curve (3) shown in figure 2 with confidence intervals estimated via bootstrapping. Note that the parameter  $c$  has a fat-tailed distribution resulting in a very high upper CI interval boundary. This is caused by the outlier behaviour of the Kachi Plain and Yellow River Valley, if they are sampled by the bootstrapping algorithm. Its 50% CI is a more robust uncertainty estimation and is given by [28.1, 61.0].

NGAs, but this time only to the central time series interval during which the  $SPC1_0$  threshold was crossed. The estimated coefficients for the full time series are used as initial values for *scipy.optimize.curve\_fit* to prevent the fitting algorithm from reversing the  $x$  direction (cf. A.1.1). The results are shown in the main part of figure 2 and parameter estimations are given in table 1.

The quality of the regression is evaluated via the coefficient of determination  $\rho^2$  in an out-of-sample prediction. The data is split randomly into equally sized training and testing data sets and a logistic regression curve  $f_i$  is estimated by only using the training data. Then,  $f_i$  is used to predict the values for the test data and the prediction is evaluated via the  $\rho^2$  metric in A.4. The random training-test-split is repeated  $i = 1, \dots, 1000$  times, each time using the estimated parameters from the full time series as initial values, and the resulting  $\rho^2$  values have an average of  $\rho^2 = 0.74 \pm 0.03$  far above 0 and their KDE distribution is shown in the inset of figure 2. This indicates a high reliability of the logistic regression model.

### 3.2 Finding a Characteristic Time Scale

Having established that the data can be accurately captured by a logistic curve, we can investigate our research question; namely, how many years did it typically take in these different regions to transition from a polity with low SPC1 to one with high SPC1? Or to reformulate the question: when does the curve leave the low plateau and when does it reach the high plateau? We attempt to answer these questions by estimating the heights of the plateaus and their respective uncertainties and by checking when the regression curve crosses these thresholds.

We performed 1000 steps of bootstrapping by sampling from the list of NGAs and by estimating the regression parameters  $(a_i, b_i, c_i, d_i)_{i=1, \dots, 1000}$  for each sample (cf. A.5). According to the asymptotic behaviour in A.1, the plateaus are given by  $b_i$  and  $a_i + b_i$ . In order to make conservative estimates instead of being influenced by noise, an upper boundary for the lower plateau's value and a lower boundary for the upper plateau's value are used as the thresholds. These thresholds are  $Th_1 = \mu(b) + \sigma(b)$  and  $Th_2 = \mu(a + b) + \sigma(a + b)$  with the empirical mean  $\mu$  and standard deviation  $\sigma$  of the bootstrapped parameters. For each bootstrapped logistic curve  $f_i(t)$ , it is then determined at which *RelTime* values  $t_1^{(i)}$  and  $t_2^{(i)}$  it crosses the lower and upper thresholds  $Th_1$  and  $Th_2$ . We can then understand the mean value

$$\mu(t_2^{(i)} - t_1^{(i)}) = \mu(t_2^{(i)}) - \mu(t_1^{(i)}) \approx 800 \text{ yr} \quad (1)$$

as the characteristic time scale for the period of rapid cultural evolution between low and high plateaus of socio-political complexity, across geography and not in reference to any specific time period. Further, a conservative upper boundary can be estimated via

$$\mu(t_2^{(i)}) + \sigma(t_2^{(i)}) - (\mu(t_1^{(i)}) + \sigma(t_1^{(i)})) \approx 1200 \text{ yr}. \quad (2)$$

These time intervals are depicted in figure 2. Note that bootstrapping has also been used to gauge the uncertainty of the parameter estimation for the logistic curve with the results shown in table 1.

#### 3.2.1 Outlier Cases

Two NGA sequences deviate significantly from the characteristic timescale identified above, as can be seen clearly in figure 2: Kachi Plain, which experiences a relatively large decline in SPC1 after an initial period of growth; and the Yellow River Valley, which exhibits a period of rapid SPC1 growth earlier than the logistic curve predicts, but then fits well with the curve after that. In the case of Kachi, which is located in modern-day Pakistan, the region experienced a fairly typical though relatively early increase in socio-political complexity during the late 3rd millennium BCE with the rise of the Harappan culture. This is captured well by the logistic



curve. Beginning around 1900 BCE, though, the region experienced a decline in complexity characterised by an abandonment of several sites, a decrease in the number typical size of settlements, diminished signs of inter-regional exchange, and a dearth of available records compared to previous periods [34, 35]. This corresponds with the 'drop' shown in figure 2. Kachi then saw a second sharp increase in SPC1 in the mid-1st millennium with the conquest of the area by the Persian Achaemenid Empire. In the Yellow River Valley (Northern China), we see an initial jump in SPC1 between the end of the Yangshao and beginning of the Longshan periods at the end of the 4th millennium BCE [36, 37, 38]. In this latter period, settlements in the area became much larger and more developed in terms of infrastructure, and we see the development of written administrative and religious texts as well as evidence for inter-regional trade [36, 39, 40]. The region then saw a steady increase in SPC1 with each culture and polity that occupied the region until the Western Han Empire. This very quick initial rise followed by an uncharacteristically long plateau of SPC1 explain the patterns seen in figure 2.

## 4 Summary and Discussion

### 4.1 Summary

Exploratory data analysis shows in figure 1 that the logistic regression is a suitable model for the *RelTime*-vs-SPC1 time series. If the data is restricted to the central part of each NGA's time series without any discontinuous polity transitions, the logistic regression is still a reasonable model as shown by its high coefficient of determination  $\rho^2 = 0.75 \pm 0.03$  for the out-of-sample prediction. Bootstrapping allows us to narrow down the time interval of rapid SPC1 growth to a maximum of 1200 years and a mean of 800 years, as highlighted in figure 2. Together, these results illustrate that there is a uniform behaviour in growth of social complexity represented by the time evolution of SPC1.

### 4.2 Validity of the Approach and Discussion on Outliers

Regarding the characteristic time scale in figure 2, it is noteworthy that the lower boundary has a larger uncertainty (light red area) than the upper boundary. This can probably be attributed to the fact that most central time series have longer intervals in the *RelTime*  $> 0$  region than in the  $< 0$  region, meaning that the upper boundary can be estimated with more data. Further, it is important to note that shifting each NGA towards *RelTime* may introduce a slight bias in the model evaluation, because the time series are already aligned via the anchor times  $T_a^{(i)}$ . This is remedied, though, by the fact that the final model is only evaluated on the central part of the time series and, therefore, the model's goodness-of-fit is not simply caused by predicting the trivial behaviour of the long tails in figure 1.

Also, the logistic curve for the central intervals shows a lower plateau and a faster growth period than the one for the full data. This may reflect the influence of discontinuous polity

changes on the SPC1 values in the non-central time series; namely, cases where an external polity conquers one of a much different SPC1 level, thus replacing the region’s SPC1 score with a significantly different value. If this is indeed the explanation for this pattern, it would suggest that in the absence of such discontinuities, many polities’ internal developments would restrict the cultural evolution to a smaller range of possible SPC1 values and that discontinuities are necessary to describe the most extreme SPC1 values and relatively fast jumps in SPC1 observed in the historical record. As an alternative explanation, disregarding the non-central time series means that with an overall less number of data points to work with, the relative influence of the outliers (seen clearly in figure 2) increases and thus, the height of the second plateau in figure 2 is pulled slightly downwards to decrease the gap between the regression curve and the Kachi Plain data. This, again, highlights the importance of further research on this topic seeking to disentangle these alternatives. The outliers to the otherwise accurate fit of this data are certainly intriguing, though having only two such cases explained by their peculiar internal developments further underscores how well the logistic curve fits the general pattern.

It is interesting to compare those NGAs that crossed the threshold  $SPC1_0$  to those that failed to do so and stayed at lower complexity values. The latter group had a median of only 3 recorded data points, i.e. there were only complex social formations coded as part of the Seshat sample for a period of roughly three centuries. On the other hand, the NGAs that did reach a high complexity and exceeded the threshold  $SPC1_0$  had a median of 38.5 recorded data points, corresponding to almost 4 millennia. Partly this is explained by different availability of historical and archaeological evidence in different regions, but it suggests also that cultural developments in the low complexity NGAs could have followed the same trajectory of logistic growth, if they had been given enough time. Unfortunately, the necessity to identify an anchor time for this analysis means that all NGAs from the Seshat world regions in North America and Oceania-Australia had to be discarded for this research. The bias introduced by this towards civilisations in Africa, Asia and Europe has to be kept in mind while interpreting our results.

### 4.3 Interpretation and Comparison to Previous Work

With the shifted time index RelTime, the logistic regression model of the SPC1 time series achieves a high accuracy. Previous work has already demonstrated a significant amount of cross-cultural generality in the factors contributing to the evolution of socio-political complexity ([6], supplemented by findings in [3, 41]). Notably, a previous study has already identified a characteristic growth pattern of SPC1 and the second principal component SPC2 and found that a rapid period of scale is first followed by a growth of information processing and economic complexity and then by further growth in scale [3]. However, the present article shows that there are not only characteristic steps of growth, but also a characteristic time interval during which growth takes place.

Our findings here expand on this prior work by identifying a that the time scales involved

in these developments also exhibit a general, characteristic shape. While the sample of past societies explored in this article is certainly not exhaustive, they comprise a fairly representative sample of regions from different parts of the world and include societies from different periods, cultures, and different developmental experiences. Our results thus lends novel empirical support to the idea (from e.g. [14, 5]) that socio-cultural evolution does indeed occur in similar time scales across different cultures and geographies. Future research can expand these insights by including additional societies and exploring alternate thresholds of complexity to identify anchor times to include more NGAs from the original sample, because the current thresholding procedure in particular excluded some NGAs from modern-day North America and Oceania-Australia from our analysis.

In terms of the underlying approach, our study tries to single out the autocatalytic effect of social complexity growth. To this end, it not only focused only on one NGA at a time, but also disregarded discontinuous changes of the polity. Thus, we uncover an empirical pattern in the temporal evolution of SPC1 that has not yet been fully discussed by previous work, e.g in causal analyses of the drivers of social complexity (e.g. [7]) and may spark further research. Our methodology differs from e.g. the regression model in [7] by deliberately choosing a very simple model to single out the temporal evolution whilst disregarding possible drivers of the observed dynamics. While the autocatalytic growth model provides an elegant interpretation of our findings (the current level of complexity facilitates further growth until the presence of an upper boundary of complexity is approached), it has to be regarded with caution: Although our model disregarded interactions with other polities, they nevertheless influence the data that was used in our sample. Previous work shows the strong effect of military conflicts with other states on the growth of sociopolitical complexity [7, 27] and even despite ignoring discontinuous polity changes, military conflicts during which the observed NGA has not been annexed are nevertheless included in the time frame of our data. Hence, the autocatalytic model might be a useful low-dimensional description of the data, but not an exhaustive explanation. In short, our findings exposes a cross-cultural temporal pattern whose causes need to be fleshed out in future work.

Finally, the findings of the present article can be used as a benchmark for future additions to the Seshat data: if a new NGA is added to the databank and shows a clear divergence from the logistic curve, it may be prudent to either check, if there are any mistakes in the data generation and interpolation, or if the divergences can be explained by historical developments like in section 3.2.1. Such a benchmark may thus be useful for further expansion of the Seshat databank.

## Author Contributions

TW performed all analyses and drafted the manuscript; DH assisted in conceptual development and drafting the manuscript.

## Acknowledgements

Initial ideas behind this paper were developed at a workshop held by the Complexity & Collapse Research Group of the Complexity Science Hub, Vienna. The authors thank all the participants at that event, particularly Mateusz Iskrzyński for valuable contributions at early stages of this project. Financial support for this work was provided by the “Complexity Science” research initiative supported by the Austrian Research Promotion Agency FFG under grant #873927 and by the German Academic Scholarship Foundation (Studienstiftung des deutschen Volkes).

## References

- [1] David Carballo, Paul Roscoe, and Gary Feinman. “Cooperation and Collective Action in the Cultural Evolution of Complex Societies”. In: Journal of Archaeological Method and Theory 21.1 (2014), pp. 98–133.
- [2] Peter J. Richerson and Morten H. Christiansen, eds. Cultural Evolution. Society, Technology, Language, and Religion. Boston: MIT Press, 2013. 499 pp.
- [3] Jaeweon Shin et al. “Scale and information-processing thresholds in Holocene social evolution”. In: Nature Communications 11.1 (May 2020), p. 2394.
- [4] Peter Turchin. Historical Dynamics: Why States Rise and Fall. Princeton University Press, 2003.
- [5] Peter Turchin and Sergey Gavrilets. “Tempo and Mode in Cultural Macroevolution”. In: Evolutionary Psychology 19.4 (2021).
- [6] Peter Turchin et al. “Quantitative historical analysis uncovers a single dimension of complexity that structures global variation in human social organization”. In: PNAS 115.2 (2018), E144–E151.
- [7] Peter Turchin et al. “Disentangling the evolutionary drivers of social complexity: A comprehensive test of hypotheses”. In: Science Advances 8.25 (2022).
- [8] Peter Turchin. “Arise 'cliodynamics'”. In: Nature 454 (2008), pp. 34–35.
- [9] Patrick Manning et al. Collaborative Historical Information Analysis. Chapter 3.09 in Reference Module in Earth Systems and Environmental Sciences, Elsevier. 2018.
- [10] V. G. Childe. Man Makes Himself. Watts & Company, 1936.
- [11] L. A. White. The Evolution of Culture. McGraw-Hill, 1959.
- [12] Elman R. Service. Origins of the state and civilization. New York, NY: WW Norton, Apr. 1975.

- [13] Patrick Vinton Kirch. “From chieftdom to archaic state: Hawai’i in comparative and historical context”. In: How Chiefs Became Kings. University of California Press, Dec. 2010, pp. 1–28.
- [14] Oswald Spengler. Der Untergang des Abendlandes. Verlag Braumüller, 1918.
- [15] David Engels. “Kulturmorphologie und Willensfreiheit”. In: Der lange Schatten Oswald Spenglers. Ed. by David Engels, Max Otte, and Michael Thöndl. Lüdinghausen: Manuscriptum, 2018, pp. 79–102.
- [16] David Engels. Oswald Spengler - Werk, Deutung, Rezeption. Stuttgart: Kohlhammer Verlag, 2021.
- [17] Oana Borcan, Ola Olsson, and Louis Putterman. “Transition to agriculture and first state presence”. A global analysis. In: Explorations in Economic History 82 (2021), p. 101404.
- [18] Elliot J. Carr. “Characteristic time scales for diffusion processes through layers and across interfaces”. In: Physical Review E 97.4 (Apr. 2018).
- [19] Eva-Maria Wartha, Markus Bösenhofer, and Michael Harasek. “Characteristic Chemical Time Scales for Reactive Flow Modeling”. In: Combustion Science and Technology 193.16 (2021), pp. 2807–2832.
- [20] Todd L. Parsons and Tim Rogers. Dimension reduction for stochastic dynamical systems forced onto a manifold by large drift: a constructive approach with examples from theoretical biology. 2015. DOI: 10.48550/ARXIV.1510.07031.
- [21] Hermann Haken. Synergetik. de. 3rd ed. New York, NY: Springer, Jan. 1990.
- [22] Peter Turchin et al. “Seshat: The Global History Databank”. In: Cliodynamics 6.1 (July 2015).
- [23] Pieter François et al. “A Macroscopic for Global History. Seshat Global History Databank: a methodological overview”. In: Digital Humanities Quarterly 10.4 (2016).
- [24] Peter Turchin et al. “An Introduction to Seshat”. In: Journal of Cognitive Historiography 5.1 (2018). Number: 1-2, pp. 115–123.
- [25] Peter Turchin et al. seshatdb (Equinox Packaged Data). Version v.1. Zenodo, June 2022. DOI: 10.5281/zenodo.6642230.
- [26] Donald B Rubin. Multiple imputation for nonresponse in surveys. Vol. 81. John Wiley & Sons, 2004.
- [27] Peter Turchin et al. “Rise of the war machines: Charting the evolution of military technologies from the Neolithic to the Industrial Revolution”. In: PLOS ONE 16.10 (Oct. 2021), pp. 1–23.

- [28] Peter Turchin et al. “Explaining the rise of moralizing religions: a test of competing hypotheses using the Seshat Databank”. In: Religion, Brain & Behavior (2022), pp. 1–28.
- [29] Peter Turchin et al. “An integrative approach to estimating productivity in past societies using Seshat: Global History Databank”. In: The Holocene 31.6 (Feb. 2021), pp. 1055–1065.
- [30] Harvey Whitehouse et al. “Testing the Big Gods hypothesis with global historical data: a review and “retake””. In: Religion, Brain & Behavior (June 2022), pp. 1–43.
- [31] Pauli Virtanen et al. “SciPy 1.0: Fundamental Algorithms for Scientific Computing in Python”. In: Nature Methods 17 (2020), pp. 261–272.
- [32] P.-F. Verhulst. “Notice sur la loi que la population poursuit dans son accroissement”. In: Corresp. Math. Phys. 10 (1838), pp. 113–121.
- [33] Daniel Hoyer. Personal communication and [http://seshatdatabank.info/browser/Seshat\\_Data\\_Browser](http://seshatdatabank.info/browser/Seshat_Data_Browser). 2022.
- [34] J. F. Jarrige. “From Nausharo to Pirak: Continuity and change in the Kachi/Bolan Region from the 3rd to the 2nd Millennium BC”. In: South Asian Archaeology 1 (1995), pp. 11–32.
- [35] Jane McIntosh. The Ancient Indus Valley: New Perspectives. Santa Barbara, CA.: ABC-Clio, 2008.
- [36] Li Liu. The Chinese Neolithic: Trajectories to Early States. Cambridge University Press, Jan. 2005. ISBN: 978-1-139-44170-4.
- [37] Anne P. Underhill. “Longshan”. In: Encyclopedia of Prehistory Volume 3. Ed. by Peter Peregrine and Melvin Ember. New York: Kluwer Academic / Plenum Publishers, 2001.
- [38] C. Zhao. “The Longshan culture in central Henan province, c. 2600–1900 BC”. In: A Companion to Chinese Archaeology. Ed. by Anne P. Underhill. Malden, MA: Blackwell, 2013, pp. 236–254.
- [39] Paola Demattè. “Longshan-era urbanism: The role of cities in predynastic China”. In: Asian Perspectives 38.2 (1999), pp. 119–153. URL: <https://www.jstor.org/stable/42928454>.
- [40] Kwang-Chih Chang, Michael Loewe, and Edward L. Shaughnessy. “China on the Eve of the Historical Period”. In: The Cambridge History of Ancient China. Cambridge University Press, 1999, pp. 37–73.
- [41] Timothy A Kohler, Darcy Bird, and David H Wolpert. “Social Scale and Collective Computation”. In: Journal of Social Computing 3.1 (2022), pp. 1–17.

- [42] David W. Hosmer and Stanley Lemeshow. Applied Logistic Regression. John Wiley & Sons, Ltd, 2000.
- [43] Emanuel Parzen. “On Estimation of a Probability Density Function and Mode”. In: The Annals of Mathematical Statistics 33.3 (Sept. 1962), pp. 1065–1076.
- [44] Murray Rosenblatt. “Remarks on Some Nonparametric Estimates of a Density Function”. In: The Annals of Mathematical Statistics 27.3 (Sept. 1956), pp. 832–837.
- [45] Bradley Efron and Robert J. Tibshirani. An Introduction to the Bootstrap. Springer US, 1994.

# Appendices

## A Methods and Technical Details

### A.1 Logistic Regression Curve

Logistic regression is used to model time series data which is mostly distributed at two plateaus with a transitory area between them [42]. It is based on the characteristic sigmoid curve of the logistic growth model described in [32], which models an exponential growth process constrained by a carrying capacity. The logistic curve has the functional form  $f$  with an asymptotic behaviour

$$f(x) = \frac{a}{1 + \exp(-c(x - d))} + b, \quad f(-\infty) = b \quad \text{and} \quad f(\infty) = a + b. \quad (3)$$

Often, data is scaled such that  $b = 0$  and  $a = 1$ , i.e. an asymptotic behaviour between two binary plateaus at height 0 and 1.

#### A.1.1 Reversing the Direction

Estimating the coefficients  $(a, b, c, d)$  can lead to numerical instabilities because it is possible to transform a logistic curve with  $c > 0$  to an equivalent equation  $\hat{f}$  with  $c < 0$ . Consider e.g.  $a = 1, b = 0, c = 1$  and  $d = 0$ , then

$$f(x) = \frac{1}{1 + \exp(-x)} = \frac{\exp(x)}{\exp(x) + 1} = \frac{\exp(x) + 1 - 1}{\exp(x) + 1} = 1 + \frac{-1}{1 + \exp(x)}. \quad (4)$$

The last reformulation of  $f$  can now be parametrised via  $\hat{a} = -1, \hat{b} = 1, \hat{c} = -1$  and  $\hat{d} = 0$ . This ambiguity can lead to the regression algorithm yielding positive and negative results for  $c$  during multiple runs. This can be prevented by setting an initial parameter guess with  $c > 0$ , which locks the algorithm into positive values for  $c$ .

### A.2 Kernel Density Estimation (KDE)

A KDE tries to reconstruct a probability density function based on a sample  $x_1, \dots, x_n$  of measurement data by smoothing the histogram of the data [43, 44]. The estimated density  $\hat{\rho}(x)$  is modelled as a weighted sum of probability densities (kernels) centred around the measured  $x_i$ . In this article, the Gaussian density is used as the kernel via `scipy.stats.gaussian_kde` [31].

### A.3 Residuals and Root Mean Squared Error

For an algorithm  $f$  which estimates values  $\hat{y}$  from data  $X$  with true values  $y$ , there are several methods to evaluate the accuracy of  $f$ . One of them is the root mean squared error  $RMSE$ .



It is defined as

$$RMSE = \sqrt{\frac{1}{n} \sum_{i=1}^n r_i^2} \quad (5)$$

via the residuals  $r_i = \hat{y}_i - y_i$ . An  $RMSE$  much smaller than the range of measured values  $y_i$  means that the model shows only little deviation from the data. A roughly symmetric distribution of the residuals around 0 indicates that the model does not have a bias towards particular values.

#### A.4 Coefficient of Prediction $\rho^2$

Another method to evaluate the quality of an estimated function  $f$  is the coefficient of prediction  $\rho^2$  used in [6]. It takes the value of  $\rho^2 = 1$ , if the prediction is always exactly true, and  $\rho^2 = 0$ , if the prediction is only as accurate as always using the mean  $\bar{y}$ . It is defined by

$$\rho^2 = 1 - \frac{\sum_{i=1}^n (\hat{y}_i - y_i)^2}{\sum_{i=1}^n (\bar{y} - y_i)^2}. \quad (6)$$

#### A.5 Bootstrapping

Bootstrapping is used to estimate standard deviations and confidence intervals in a model-free approach. A sample  $z_1, \dots, z_n$  is re-sampled *with* replacement, i.e. a new sample  $\tilde{Z} = z_{i_1}, \dots, z_{i_n}$  is created that for some  $j \neq k$  fulfils  $i_j = i_k$ . This procedure is repeated  $N$  times so that there are  $\tilde{Z}_1, \dots, \tilde{Z}_N$  bootstrapped samples. If  $N$  is large enough, then e.g. the mean  $\tilde{\mu}(z)$  of the re-sampled data will converge to the true mean of the original sample, but the empirical distribution of the re-sampled means  $\tilde{\mu}_1(z), \dots, \tilde{\mu}_N(z)$  enables the calculation of the confidence interval of the empirical mean [45]. This approach can be adapted to make inference on the standard deviation and CIs of any statistical property of the original sample.

## B Example of the Data Preprocessing

We illustrate the preprocessing of the raw SPC1 time series using the NGA 'Latium' (modern day central Italy) as an example. Figure 3 shows the shift between the original time series to the *RelTime* time frame relative to the anchor time  $T_a^{(Latium)} = 700$  BC. Figure 4 shows how the SPC1 time series of Latium is dissected into three intervals based on the discontinuous polity changes based on the establishments of the Roman Principate (from the republic to an empire) and of the Republic of St. Peter (Papal States). Note that the time index is given in *RelTime* and that the "central" time series actually includes all data to the left of the first recorded discontinuous transition because there is no discontinuous transition before reaching the threshold value  $SPC1_0$ .

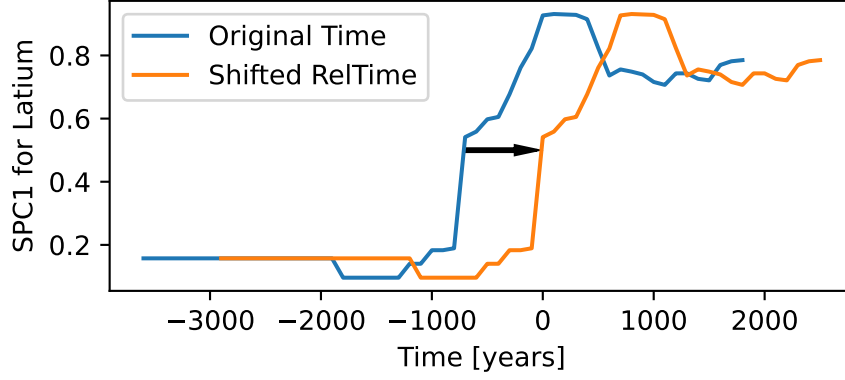


**Figure 3:** Illustration of how the SPC1 time series of the Latium NGA is shifted by its anchor time to the new relative time frame *RelTime*. Hence, at *RelTime* = 0, the shifted time series is equal to the threshold value  $SPC1_0$ .

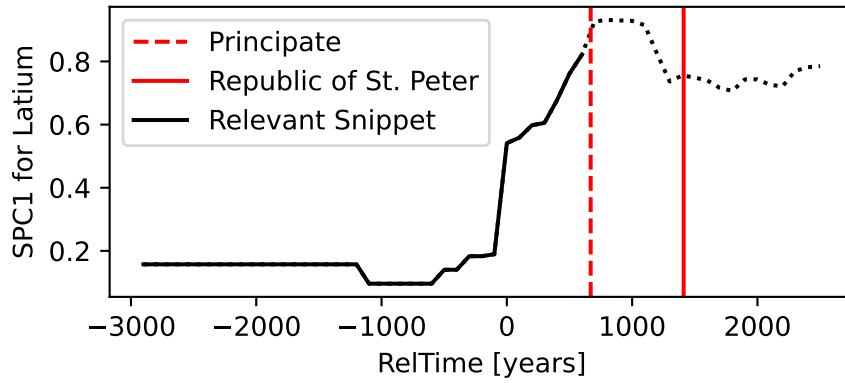


**Figure 4:** The two recorded discontinuities for the Latium NGA (red) are used to divide its SPC1 time series into different intervals. The interval containing the threshold value  $SPC1_0$  (the "Relevant Snippet" with the solid line) is used for further analysis whereas the rest (dotted) is discarded. Note that the times of the discontinuities do not line up with the 100-year time intervals of the SPC1 measurement which is why parts of the dotted line are to the left of the first discontinuity's vertical line.